Geophysical Research Letters

RESEARCH LETTER
10.1029/2023GL104759

Key Points:

- The South Qiangtang block was located at ~30°N in the Late Triassic
- In the Permo-Triassic the South Qiangtang block drifted rapidly northward at ~13.4 cm/yr
- The Longmuco-Shuanghu Ocean closed no later than ca. 222 Ma

Supporting Information:

Supporting Information may be found in the online version of this article.

Correspondence to:

X. Cheng and H. Wu,
chengxin@nwu.edu.cn;
wuhn2506@nwu.edu.cn

Citation:

Wei, B., Cheng, X., Domeier, M., Zhou, Y., Chen, Q., Jiang, N., et al. (2023). Paleomagnetism of late Triassic volcanic rocks from the south Qiangtang block, Tibet: Constraints on Longmuco-Shuanghu Ocean closure in the Paleo-Tethys Realm. *Geophysical Research Letters*, *50*, e2023GL104759. https://doi.org/10.1029/2023GL104759

Received 2 JUN 2023
Accepted 26 SEP 2023

Paleomagnetism of Late Triassic Volcanic Rocks From the South Qiangtang Block, Tibet: Constraints on Longmuco-Shuanghu Ocean Closure in the Paleo-Tethys Realm

Bitian Wei[1], Xin Cheng[1], Mathew Domeier[2,3], Yanan Zhou[1], Qinglong Chen[1], Nan Jiang[4], Longyun Xing[1], Dongmeng Zhang[1], Teng Li[1], Feifan Liu[1], Jiahui Zhang[1], and Hanning Wu[1]

[1]State Key Laboratory of Continental Dynamics, Department of Geology, Northwest University, Xi'an, China, [2]Centre for Earth Evolution and Dynamics (CEED), University of Oslo, Oslo, Norway, [3]Centre for Planetary Habitability (PHAB), University of Oslo, Oslo, Norway, [4]School of Petroleum Engineering and Environmental Engineering, Yan'an University, Yan'an, China

Abstract The South Qiangtang block of the Qinghai-Tibet Plateau represents an area critical to understanding the late Paleozoic and early Mesozoic history of the Tethyan realm, but its drift history remains poorly constrained. Here we report a new quantitative paleogeographic constraint for the South Qiangtang block from a paleomagnetic study of Late Triassic volcanic rocks of the Xiaoqiebao Formation. A characteristic remanent magnetization isolated from 25 sites passes both fold- and reversal tests, and likely represents a primary magnetization. On the basis of these data, we estimate that the South Qiangtang block occupied a paleolatitude of 30.1 ± 4.6°N at ca. 222 Ma. When combined with existing paleomagnetic constraints, these new results indicate that the South Qiangtang block (and other "Cimmerian" blocks) moved rapidly northward (in true latitude) between the middle Permian and Late Triassic. Our new data further suggest that the southern branch of the Paleo-Tethys (Longmuco-Shuanghu Ocean) likely closed by the mid-Late Triassic.

Plain Language Summary The Paleo-Tethys was a major eastward-widening oceanic domain that separated eastern Gondwana and eastern Laurasia during Carboniferous-Permian time. The eventual disappearance of this ocean coincided with the amalgamation of the terranes comprising the modern Qinghai-Tibet Plateau. However, the plate kinematic history that led up to this suturing remains poorly constrained. In particular, the South Qiangtang block, which is thought to have formed the southern margin of the system, is a key area in need of additional constraints. In this work, we present new paleomagnetic results which indicate that the South Qiangtang block drifted rapidly northward between the middle Permian and Late Triassic (at an average south-north speed of ~13.4 cm/yr) to arrive to a paleolatitude of 30°N by 222 Ma. Such a position suggests that the southern branch of the Paleo-Tethys (Longmuco-Shuanghu Ocean) may have closed by this time.

1. Introduction

The Paleo-Tethys Ocean was a major eastward-widening ocean that divided eastern Laurasia and eastern Gondwana in Carboniferous-Permian time (e.g., Metcalfe, 2013; Stampfli et al., 2013; Torsvik & Cocks, 2013; Torsvik et al., 2012; Zhao et al., 2018). According to conventional paleogeographic models, in the latest Paleozoic and early Mesozoic the Paleo-Tethys progressively shrank due to the northward drift of a series of crustal blocks that rifted from the northern margin of Gondwana (the "Cimmerian" continent or terranes, including the Qiangtang block(s), Sibumasu, Iran block, Afghanistan, and others) (Angiolini et al., 2013; Song et al., 2017; Stampfli & Borel, 2002; Wan et al., 2019; Şengör et al., 1988), and the ocean finally closed by the collision and amalgamation of those terranes with the southern margin of Eurasia (Li et al., 2009, 2019; Pullen et al., 2008; Wang et al., 2018; Xu et al., 2015; Zhao et al., 2018). However, despite the attractiveness of this simplistic paleogeographic narrative, closure of the Paleo-Tethys was likely not a singular event, as multiple corridors proposed to be sutures crossing the Qinghai-Tibet Plateau have been related to the "Paleo-Tethys." Because the collapse of this once-massive oceanic domain is central to an understanding of the tectonic evolution of central Asia, as well as the regional environmental and biogeographic setting in the late Paleozoic and early Mesozoic, it is important to unravel the detailed internal kinematics of its demise.

Proposed "Paleo-Tethys" sutures include the East Kunlun-Animaqing suture (EKAS) that broadly demarcates the southern margin of Tarim and Qaidam, the Xijinwulan-Jinshajiang suture (XJS) that forms the northern border of the North Qiangtang block (NQB) and the Longmuco-Shuanghu suture (LSS), which separates the NQB and South Qiangtang block (SQB), (e.g., Chang & Zheng, 1973; Kapp et al., 2000, 2003; Li, 1987; Liu et al., 2019; Li, Zhai, Dong, Zeng, & Huang, 2007; Metcalfe, 2013; Pan et al., 2004; Pullen et al., 2008; Yin & Harrison, 2000) (Figure 1a). These various sutures may represent different "branches" of the Paleo-Tethys, which should thus be treated as an oceanic realm rather than a singular basin. Following this, the EKAS and XJS represent a composite northern branch—the "Jinshajiang Ocean" (JSO), whereas the LSS is interpreted to mark a distinct southern branch—the "Longmuco-Shuanghu Ocean" (LSO) (Wu et al., 2020; R. X. Zhu et al., 2022).

Paleomagnetic and geologic data suggest that the JSO narrowed with the rapid northward drift of the NQB during the late Permian to Triassic, and closed by the collision of the NQB with the southern margin of Laurasia by the early Late Triassic (Cheng et al., 2023; Guan et al., 2021; Yu et al., 2022). However, the evolution of the LSO remains less clear (e.g., Li, 1987; Zhang, Zhang, et al., 2006; Y. C. Zhang et al., 2016; Yin & Harrison, 2000; Kapp et al., 2003; Gehrels et al., 2011) and proposals of its closure time range from the late Permian to the Late Triassic (e.g., Qi et al., 2009; Xie et al., 2018; Yang et al., 2011; Zhai et al., 2018). As the SQB represents the southernmost block of the Qinghai-Tibet Plateau that once bounded the LSO, constraints on the latest Paleozoic to early Mesozoic drift history of this block are needed to constrain the evolutionary collapse of the LSO, and thus the Paleo-Tethys realm more broadly. However, late Paleozoic-early Mesozoic quantitative paleomagnetic constraints on the SQB are presently very sparse (Wei et al., 2022).

Here we report on new paleomagnetic data collected from Late Triassic volcanic rocks from the SQB. Combined with existing Permian paleomagnetic data, we apply these new data to further constrain the drift history of the SQB during the latest Paleozoic-early Mesozoic, in order to further constrain the kinematic evolution of Paleo-Tethys closure.

2. Geological Setting and Sampling

The sampling area of this study is located in the centeral part of the northern margin of the SQB, 50 km south of the LSS, near Xiaochaka Lake and Pengyan Co Lake, in Shuanghu County (Figure 1b). In this area, Late Triassic strata are widespread and observed to overlie late Carboniferous rocks with angular unconformity. Contacts between Late Triassic strata and Permian and Jurassic strata are exclusively faulted (Figure 1b). The Late Triassic successions comprise, from bottom to top: the Xiaoqiebao Fm. (also called the Nadigangri Fm. by Li (2019)), Jiangzhong Fm., Jiaomuchaka Fm. and Zhana Fm. (Figure 1b). The Jiangzhong Fm., Jiaomuchaka Fm., and Zhana Fm. are mainly composed of limestone and sandstone, whereas the Xiaoqiebao Fm. is a bimodal volcanic sequence (Li, 2019). The latter is mainly comprised of grayish green or purple amygdaloidal basalt, basaltic andesite, basaltic breccia, and rhyolite. Limestones have also been reported to occur among the volcanics of the Xiaoqiebao Fm. (Feng et al., 2005), but we did not observe any interlayered limestones in the sampling area. Geochemically, the Xiaoqiebao volcanics have been associated with a rift-related intra-plate extensional environment (Fu et al., 2010a, 2010b; Li, 2019; Wang et al., 2022). A K-Ar date of 223 ± 5 Ma is reported from volcanic rocks of the Xiaoqiebao Fm. in the study area (Wang, Qu, et al., 2007; Figure 1b), and Li (2019) reported zircon U-Pb ages of 221.9 ± 3.4 Ma (MSWD = 1.6) near the Xiaochaka lake and 221.8 ± 2.1 Ma (MSWD = 0.8) from the Jianshishan section. We thus calculate the average age of the Xiaoqiebao Fm. as 222.0 ± 3.3 Ma. A Late Triassic age is further supported by sporopollen (*Schizosporites* cf. *parvus*, *Psophosphaera bullulinaeformis*, *Cycadopites* sp., *Chasmatosporites* sp., *Megamonoporites cacheutensis*, *Megamonoporites* sp.) and bivalve (*Halobia* sp., *Burmesia* sp., *Chlamys* sp.) fossils found among limestone interlayers of the Xiaoqiebao Fm. (Feng et al., 2005). The bottom boundary of the Xiaoqiebao Fm. in the study area is a paleo-weathering crust (Fu et al., 2009; Wang, Fu, et al., 2007; Wang et al., 2022) that regionally mantles the Carboniferous-Permian strata (Fu et al., 2009, 2010a; Zhu et al., 2005).

Structurally, the study area exhibits clear evidence of several episodes of Mesozoic and Cenozoic tectonism. The pre-Late Triassic angular unconformity capped by a paleo-weathering crust, together with the absence of Early and Middle Triassic strata, indicates that the region was deformed and uplifted in Early to Middle Triassic time (Wang & Fu, 2018). The Late Triassic and Jurassic strata in the study area mostly strike ESE-WNW and dip both to the SSW and NNE. In the northeast of the study area, near Kongkongchaka Lake, the Late Triassic strata are disconformably overlain by Early-Middle Jurassic strata (Wang et al., 2022). The occurrence of another

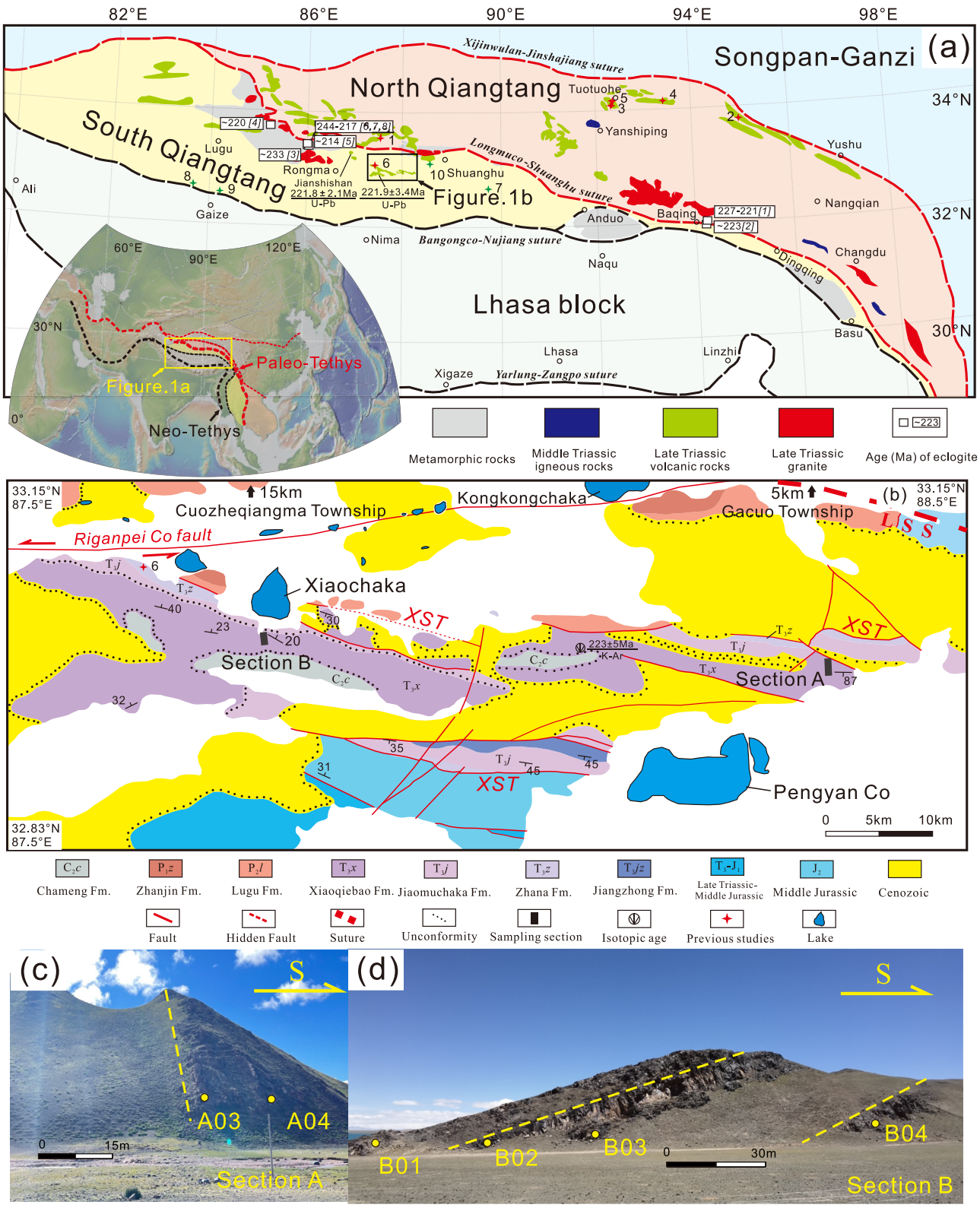

Figure 1.

angular unconformity between Jurassic and Cenozoic strata reflects another episode of compressional deformation and regional uplift that is ascribed to the collision of Lhasa against the SQB (marking the closure of the Bangongco-Nujiang Ocean) in late Early Cretaceous to early Late Cretaceous time (Liu et al., 2001, 2002; Wu et al., 2011, 2012; Ren et al., 2016; Li et al., 2017; Zhao et al., 2019a, 2019b; Cao et al., 2020; Ma et al., 2023). Subsequently, during the Cenozoic Himalayan orogeny, the collision of India against Eurasia resulted in another strong compressional episode in the SQB, and the development of large-scale WNW-trending thrust structures (e.g., Xiaochaka-Shuanghu thrust) and transcurrent structures (e.g., Riganpei Co left-lateral strike-slip fault) (Figure 1b; Liu et al., 2022).

Paleomagnetic samples were collected from two sections, here called Section "A" (33°N, 88.4°E) and Section "B" (33°N, 87.8°E) (Figure 1b). In Section A, the volcanic rocks dip ~87° to the south, whereas in Section B the volcanic rocks dip 17–28° to the north. In Section A, 114 samples from 13 sites were drilled from grayish green basalt, purplish red basaltic andesite and red rhyolite (Figure 1c). In Section B, 91 samples from 12 sites were drilled from grayish green basalt. In both sections, a "site" represents a distinct volcanic flow (Text S1 in Supporting Information S1), which could be distinguished by lithological and textural variations (e.g., quenched margins; Figures S1a and S1b in Supporting Information S1), and paleohorizontal was estimated from flow structures (Figures S1c–S1f in Supporting Information S1). Samples were collected using a gasoline-powered drill and were oriented in situ using magnetic and solar compasses (yielding an uncertainty of <5°). A handheld GPS unit was used to determine the geographic coordinates of the sampling sites, and structural orientations were measured with a magnetic compass.

3. Results

Detailed rock-magnetic experimental methods, their results and scanning electron microscopy observations are presented in Text S2 in Supporting Information S1, and paleomagnetic methods are presented in Text S3 in Supporting Information S1; in the following we summarize the key results. On the basis of our rock magnetic experiments, we interpret both magnetite and hematite to be the main magnetic carriers in the samples from Section A, whereas in Section B the main magnetic carrier is magnetite alone.

In section A, the demagnetization curves of most specimens typically exhibit two-component behavior: a low-temperature remanent component (LTC) was removed by approximately by 350°C, and a high-temperature component (HTC) was isolated between 350 and 585°C or 350 and 680°C (Figures 2a and 2b); we deem the HTC the characteristic remanent component (ChRM). In some specimens little decay occurred below 350°C, and only the high-temperature ChRM could be defined (Figure 2c). In section B, all specimens display two components of magnetization: a LTC removed below 350°C gives way to a high-temperature component that decays univectorially to the origin between 350 and 585°C (Figures 2d). Although we found thermal demagnetization (TD) to be most effective, experiments with alternating field demagnetization (AF) and hybrid (AF + TD) treatments yielded results consistent with those described above (Figures 2e and 2f). The ChRM data of the individual samples are provided in Table S1 (Wei, 2023).

The directions of the LTC from both sections are similar, and a mean calculated from 161 samples is $D_g = 356.4°$, $I_g = 51.1°$, $k_g = 9.8$, $\alpha_{95g} = 3.7°$ in geographic coordinates and $D_s = 12.5°$, $I_s = 82.9°$, $k_s = 1.9$, $\alpha_{95s} = 11.8°$ after tilt correction. In geographic coordinates, the mean direction is close to the direction of the present geomagnetic field ($D = 0.7°$, I = 51.9). Furthermore, the dispersion of the LTC directions increases significantly with tilt correction (Figures 2g and 2h). Stepwise tectonic correction of the LTC (Watson & Enkin, 1993) yields an optimal clustering at $-11.4 \pm 1.5\%$ unfolding, indicating that the magnetization post-dates folding and is thus a remagnetization (Figure 2i).

In geographic coordinates, the ChRM directions from both sections are south-pointing, but have inclinations of opposite sign (Figure 2j). The mean ChRM direction computed from the 13 Section A sites is $D_g = 196.6°$,

Figure 1. (a) Simplified regional geological map showing the locations of the Triassic igneous rocks in Qiangtang (modified after Li et al. (2019) and He et al. (2022)). Red crosses depict the location of Triassic paleomagnetic studies: 1-Song et al. (2012); 2-Yu et al. (2022); 3-Song et al. (2015); 4-Lin and Watts (1988); 5-Zhou et al. (2019); 6-Song et al. (2012). Green crosses depict the locations of Jurassic-Cretaceous paleomagnetic studies: 7-Cao et al. (2019); 8-Cao et al. (2020); 9-Chen et al. (2017); 10-Meng et al. (2018). White squares are the age of eclogite: 1-Jin et al. (2019); 2-X. Z. Zhang et al. (2018); 3-Dan et al. (2018); 4-Zhai et al. (2011); 5-Zhang et al. (2010); 6-Zhai et al. (2017); 7-Pullen et al. (2011); 8-Pullen et al. (2008). (b) Regional geological map showing the sampling section (modified after Jiangaidarina, and Paduco regional geological survey reports). LSS: Longmuco - Shuanghu Suture; XST: Xiaochaka-Shuanghu thrust. (c–d) Photographs of the Triassic volcanic rocks in Section A and Section B.

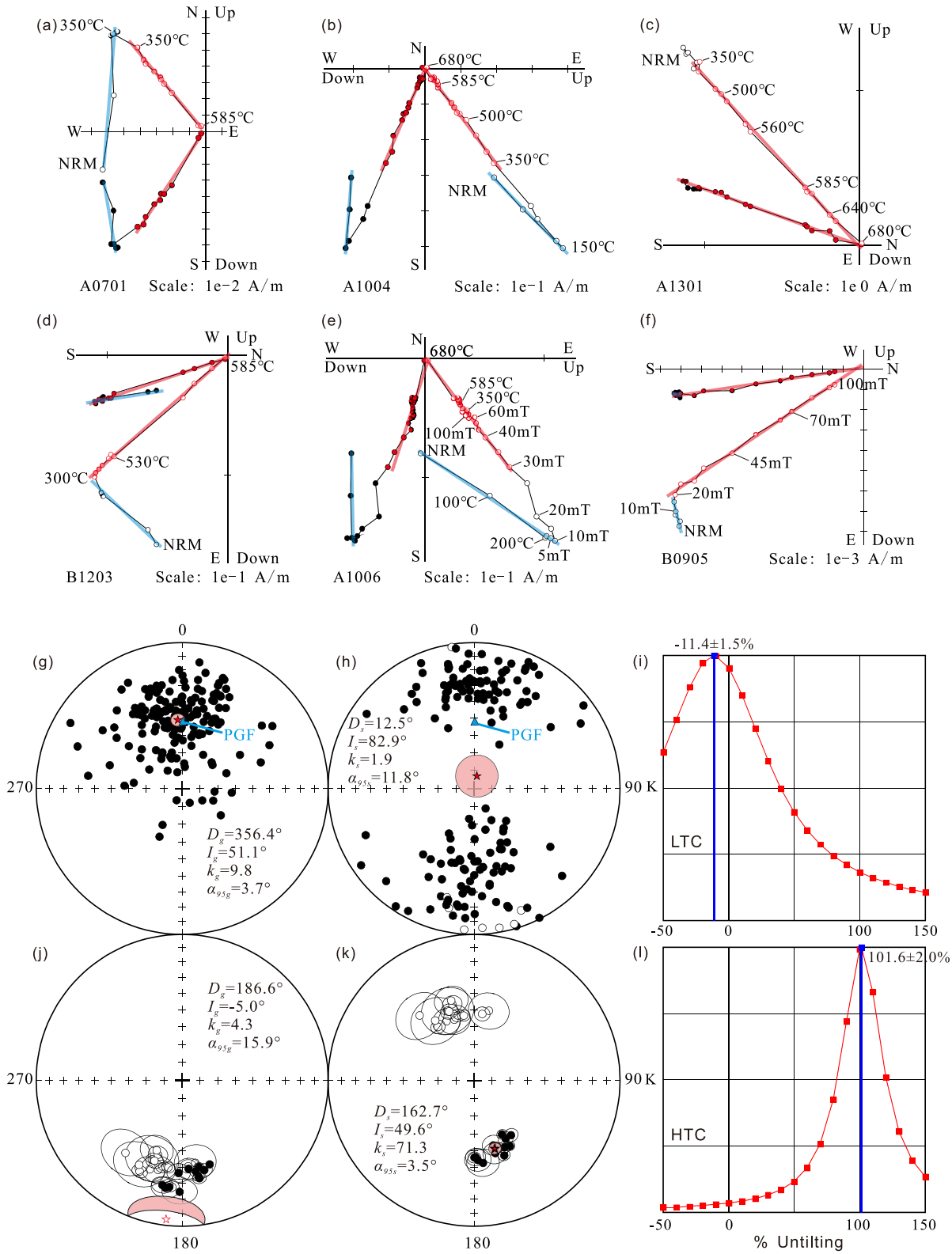

Figure 2.

$I_g = -40.1°$, $k_g = 60.4$, $\alpha_{95g} = 5.4°$ in geographic coordinates and $D_s = 342.2°$, $I_s = -50.3°$, $k_s = 60.1$, $\alpha_{95s} = 5.4°$ after tilt correction, and from the 12 section B sites is $D_g = 176.6°$, $I_g = 33.7°$, $k_g = 70.0$, $\alpha_{95g} = 5.2°$ in geographic coordinates and $D_s = 163.2°$, $I_s = 48.8°$, $k_s = 81.9$, $\alpha_{95s} = 4.8°$ after tilt correction. With tilt-correction, Section A directions become north-pointing, approximately antipodal to those of Section B. Accordingly, after tilt-correction, we find that the ChRMs of sections A and B pass the McFadden and McElhinny (1990) and Heslop and Roberts (2018) reversal tests (Table S2; Wei, 2023). The execution of several fold tests on these 25 ChRMs (after inverting them to a common polarity) also yielded positive results at the 99% confidence level, with optimal clustering occurring at 101.6 ± 2.0% unfolding (Figure 2l and Table S2; Wei, 2023).

Given the results of the fold and reversal tests, which establish that the ChRMs of the two sections share a common mean and pre-date folding, we merge the directions from the 25 sites and calculate a mean, tilt-corrected direction of $D_s = 162.7°$, $I_s = 49.6°$, $k_s = 71.3$, $\alpha_{95s} = 3.5°$ (Figure 2k). An alternative mean computed from 199 specimen-level directions is $D_s = 162.8°$, $I_s = 49.7°$, $k_s = 37.6$, $\alpha_{95s} = 1.6°$, which is not significantly different than the mean computed from site level directions. After transforming each of the 25 site means into virtual geomagnetic poles (VGPs), we compute a corresponding paleomagnetic pole at $\lambda = -24.4°$N, $\varphi = 104.5°$E, $A_{95} = 4.3°$. With respect to theoretical expectations for paleosecular variation (PSV), this pole meets the N-specific criterion of Deenen et al. (2011) (critical A_{95} values of 3.5–6.9° for $N = 25$), which suggests that PSV has largely been averaged out.

4. Discussion

4.1. Age of the Magnetization and the Paleolatitude of the SQB During Late Triassic

The result of the fold test clearly demonstrates that the age of the ChRM isolated from the Xiaoqiebao Fm. volcanic rocks pre-dates the age of the folding of those rocks. The most recent deformation episode to have affected the Triassic strata can be associated with the Cenozoic collision of India against Eurasia (Zhao et al., 2019, 2019a, 2019b), which at least constrains the timing of ChRM acquisition to the pre-Paleogene. However, the angular unconformity between the Jurassic and Cenozoic strata (and the general sparsity of Cretaceous strata in the region) indicates that significant deformation also occurred during the earlier Cretaceous collision of Lhasa against the SQB, and so we may further infer that the ChRM is pre-Cretaceous in age. Given that the ChRM is associated with antipodal directions held in different minerals from several lithologies, we contend that the magnetization is most likely primary.

The only other Late Triassic paleomagnetic constraint from the SQB is from the Zhana Fm. sandstone, as reported by Song et al. (2012), but this constraint has a significant shortcoming. Being derived from clastic sedimentary rocks, the paleomagnetic inclinations may have been flattened, but Song et al. (2012) did not conduct any tests to evaluate this potential bias. In this regard it is worth noting that our mean paleomagnetic direction is steeper than that of Song et al. (2012) (Figures 3a and 3b). Owing to this important but unquantified potential bias, we do not further consider this constraint.

The position of our new pole differs from existing post-Late Triassic poles reported from the SQB (Figure 3a; Text S4 in Supporting Information S1). Normally this could be used as an additional argument against remagnetization, but these younger paleomagnetic poles are distributed about a small circle centered on the sampling area, which suggests that significant vertical-axis rotations have occurred within the SQB since the Late Triassic (Figure 3a). Meng et al. (2018) likewise concluded from paleomagnetic data that a clockwise vertical-axis rotation of 57.3 ± 3.9° (relative to stable Eurasia) occurred in the Shuanghu basin since mid-Cretaceous time. However, note that even paleomagnetic data of similar age from the same region appear to have been significantly rotated relative to one another (e.g., Chen et al., 2017). Such rotations could have been caused by the Lhasa-SQB collision (e.g., Kapp et al., 2007; Liu et al., 2017; Hu et al., 2022; Z. C. Zhu et al., 2022) during the Cretaceous, but the dispersion of Late Cretaceous poles and the occurrence of large scale strike-slip faults associated with the India-Eurasia collision indicates this latter event was also a major contributor (e.g., Ding et al., 2005, 2022; Hu

Figure 2. (a–f) Representative demagnetization results of samples from the Xiaoqiebao Formation (shown in geographic coordinates). The colored circles and colored straight lines represent the points involved in the PCA and the fitted direction, respectively. Blue (red) corresponds to the low-temperature components (high-temperature components). Equal-area projection of the low-temperature component and high-temperature component before (g and j) and after (h and k) tilt correction. The blue triangle is the mean direction of the local present geomagnetic field (PGF) and the red star within the pink circle is the mean direction and its α_{95}. Open (filled) circles/stars are projections onto the upper (lower) hemisphere. (i and l) Partial untilting test (Watson & Enkin, 1993) of LTC and HTC. The red line shows the precision parameter k as a function of untilting, and the blue line marks the percent untilting that maximizes the precision parameter.

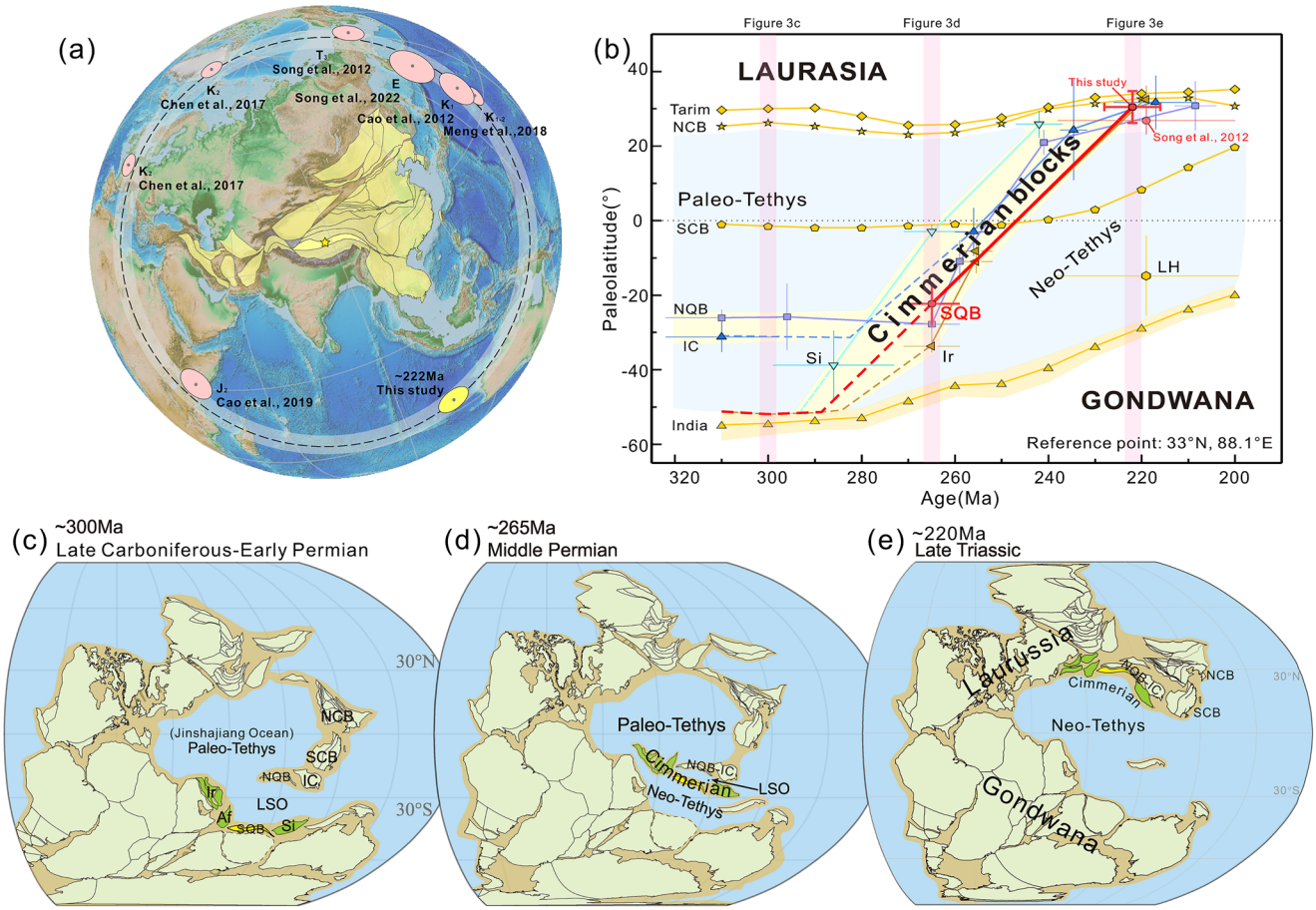

Figure 3. (a) Plot of post-Triassic paleomagnetic poles from SQB. Yellow star: sampling location; circles: Mesozoic paleomagnetic poles of SQB (Table S3 in Wei (2023)); light gray band: the error bounds of our new pole as a small circle centered on sampling site; (b) Paleolatitude evolution of the SQB and its surrounding blocks during the early Permian to Late Triassic (modified after Wei et al. (2022); the paleolatitude evolution of the North Qiangtang Block is modified after Cheng et al. (2023); see Table S3 for detailed paleomagnetic data). (c) Paleogeographic reconstructions of the SQB during the Early Permian to Late Triassic (modified after Huang et al., 2018; Yan et al., 2019; Wei et al., 2022).

et al., 2016; Jin et al., 2018; Suo et al., 2022). Because the sampling area may have suffered vertical-axis rotations, the declination of our reported ChRM should not be used for paleogeographic reconstruction, and we rely only on the inclination. The inclination indicates that the SQB was located at a latitude of 30.1 ± 4.6° at ~222 Ma.

4.2. The Permian to Triassic Drift History of SQB

Several lines of geological evidence suggest that the SQB was proximal to Sibumasu and the northern margin of Gondwana in the Permo-Carboniferous, including the occurrence of glacial relics (e.g., Li, 1987; Wang et al., 2021) and the provenance (age distribution and isotopic signature) of detrital zircons (e.g., Fan et al., 2015; Gao et al., 2022). An early Permian paleomagnetic result from Sibumasu places it at 40°S (Huang & Opdyke, 1991; Xu et al., 2015), which is consistent with it being positioned along the northern margin of Gondwana then (Figure 3c). By contrast, paleomagnetic constraints from Indochina (IC) and the North Qiangtang block (NQB) indicate that they occupied distinctly lower latitudes in the Permo-Carboniferous (~20°S; Cheng et al., 2012; Song et al., 2017; Yang et al., 2017; Yan et al., 2020; Cheng et al., 2023), as also reflected by their very different (warm water) faunas (Y. C. Zhang et al., 2016). On the basis of these sparse paleomagnetic constraints, we estimate that the width of the LSO (between SQB-Sibumasu and IC-NQB) was on the order of ~2,000 km at this time, while the JSO (between IC-NQB and Tarim-North China Block) exceeded 5,000 km (Figure 3c). Thus, the latter can most appropriately be considered the "main" Paleo-Tethys Ocean, although the LSO may have provided an important oceanic gateway connecting the Tethyan and Panthalassic realms.

In the early Permian, a large-scale episode of dyke emplacement occurred along the northern margin of Gondwana, which may have been associated with a mantle plume (Zhai et al., 2013a; Y. X Zhang et al., 2018; Wang et al., 2019; Dan et al., 2021). In turn, that magmatism may have facilitated the disintegration of the northern margin of Gondwana by the breakout of numerous crustal blocks (Wang et al., 2019; Zhai et al., 2013a) that were already subject to tension imparted by the northward subducting Paleo-Tethys (Wan et al., 2019, 2021; Wu et al., 2020; R. X. Zhu et al., 2022; Zhu et al., 2023). The rifting of those crustal blocks (the "Cimmerian" blocks) from the northern margin of Gondwana marked the opening of the Neo-Tethys Ocean, which proceeded to widen as the crustal blocks drifted north. Northward migration of the SQB at this time is supported by its assemblage of middle Permian fossils, which reflect a transition from Gondwanan to Cathyasian faunal affinities (Shen et al., 2016; Zhang et al., 2014). More quantitatively, a middle Permian paleomagnetic result from the SQB places it at ~22°S then (Wei et al., 2022). Contemporaneous paleomagnetic data from the IC-NQB suggest they remained at low latitudes during the middle Permian, and so the LSO would have narrowed (as the Neo-Tethys grew), while the JSO remained wide (Figure 3d).

Our new paleomagnetic results indicate that in the Late Triassic the paleolatitude of the SQB was 30.1 ± 4.6° (Figure 3b). Although these data do not constrain the hemisphere, geological evidence that the NQB and SQB amalgamated in the Late Triassic (see next section) would suggest that the SQB laid at 30°N at this time (provided that the paleolatitude of NQB was ~32°N by ~227–222 Ma; Yu et al. (2022)). Comparing this ~222 Ma paleolatitude constraint with the ~265 Ma constraint (~22°S; Wei et al., 2022) allows the determination that the SQB must have drifted northward at a minimum average rate of 13.4 cm/yr between those times (Figure 3b). Middle Permian to Late Triassic paleomagnetic constraints from the Iranian block, another of the Cimmerian blocks, reflect a similarly rapid rate of northward drift (10–14 cm/yr) during this interval (Besse et al., 1998), when the NQB-IC also experienced rapid northward movement (Cheng et al., 2023; Ma et al., 2019; Yan et al., 2019; Zhou et al., 2019) (Figure 3b). Hence, this was a dynamic interval that witnessed swift plate motions and the rapid expansion of the Neo-Tethys Ocean at the expense of the Paleo-Tethys.

4.3. Ocean Closures in the Paleo-Tethys Realm

The main cratons of the East Asia continental collage (e.g., Tarim, North China Block and South China Block) are thought to have mostly assembled and collided with the north Eurasian body of the Pangea supercontinent by the mid-Late Triassic (Huang et al., 2018; Zhao et al., 2018). Late Triassic paleomagnetic data from the central-eastern NQB (Song et al., 2015; Zhou et al., 2019), eastern NQB (Yu et al., 2022) and northern IC (Yan et al., 2019) likewise suggest that the IC-NQB collided with the southern margin of the East Asian collage about the same time, at ~230 Ma (Yu et al., 2022). This implies that the northern branch of the Paleo-Tethys (the JSO) closed during the early Late Triassic (Figure 3e).

The existence of a southern branch of the Paleo-Tethys (the LSO) is supported by geologic evidence including Late Devonian radiolarian fauna (Li et al., 2024) and Cambrian to Permian age ophiolitic mélange exposed along the LSS (e.g., Hu, Li, Wu, et al., 2014; Zhai, Jahn, Wang, et al., 2013; Zhai et al., 2016; X. Z. Zhang et al., 2016; T. Y. Zhang et al., 2018), but the timing of its closure remains unclear. Previous proposals of LSO closing time span a range of intervals: late Permian—Early Triassic (Qi et al., 2009; Yang et al., 2011), Early Triassic (Xie et al., 2018), Middle Triassic (Hu, Li, Li, et al., 2014; Peng et al., 2015; Pullen et al., 2008; Wang et al., 2011) and Late Triassic (Dan et al., 2018; Dong et al., 2013; Li, Zhai, Dong, Yu, & Huang, 2007; Song et al., 2015; Zhai et al., 2011, 2018).

Our new paleomagnetic paleolatitude constraint supports the notion that the NQB and SQB merged into a unified whole by at least the mid-Late Triassic, given that they occupied similar latitudes by then (Figure 3b). Notably, this inference is based on the simplistic premise that the NQB and SQB occupied the same longitude at that time. It is therefore important to consider this interpretation (that the Paleo-Tethys ocean had closed at least by mid-Late Triassic time) against the geologic evidence. In the following we briefly review some key regional stratigraphic, metamorphic and geochemical observations.

Starting with a stratigraphic perspective, a key observation is that Early-Middle Triassic strata are absent across large areas of the SQB (including our sampling area), and the Late Triassic strata rest atop late Paleozoic rocks above a regional angular unconformity. This unconformity suggests that the SQB was uplifted and denuded in the Early to Middle Triassic (Wang & Fu, 2018), possibly resulting from terrane collision associated with Paleo-Tethys closure (Wang et al., 2022; Yan et al., 2016; Zhai et al., 2011). Similarly, in the middle of the LSS,

unmetamorphosed continental sediments of the ca. 214 Ma Wanghuling Fm. rest with angular unconformity above late Paleozoic metamorphic rocks and ophiolite remnants (Li, Zhai, Dong, Yu, & Huang, 2007). The Wanghuling Fm. is recognized as the oldest continental sedimentary sequence covering the ophiolitic mélange in the LSS, which thereby places a minimum age on LSO closure.

The occurrence of high-pressure/low-temperature (HP-LT) metamorphic rocks in the LSS also provide important information about the closure of the LSO by way of the corresponding continental collision. Along the LSS, Late Triassic HP-LT metamorphic rocks form a >500 km long and up to 100-km wide belt that was generated by the partial subduction of oceanic crust and associated metasedimentary rocks during terminal closure of the LSO (Figures 1a and 3d; e.g., Kapp et al., 2000; Zhang, Cai, et al., 2006; Zhang, Fan, et al., 2018; Li, 2008; Dong & Li, 2009; Li et al., 2009; Zhang & Tang, 2009; Zhang et al., 2010; Zhai et al., 2011; X. Z. Zhang et al., 2018; Jin et al., 2019). More specifically, the peak (eclogite-facies) HP metamorphic stage interpreted to closely post-date terminal LSO closure has been estimated to ca. 227–223 Ma, whereas the subsequent cooling stage recording exhumation of the metamorphic rocks during post-collisional extension has been estimated to ca. 223–214 Ma. (Dan et al., 2018; Tang & Zhang, 2014; X. Z. Zhang et al., 2018; Y. X. Zhang et al., 2018; Zhai et al., 2011, 2017). These constraints again suggest that the LSO had closed no later than the mid-Late Triassic (Figure 3e).

A Late Triassic closure of the LSO is also supported by some geochemical evidence. During the Late Triassic the LSS was extensively intruded by granites that yield geochemical signatures interpreted as "post-collisional" (Figure 1a; e.g. Dong et al., 2013; Fu et al., 2010a, 2010b; Hu et al., 2010, 2014a; Li et al., 2015; Ma et al., 2016; Wang et al., 2015; Peng et al., 2015; Qian et al., 2016; Shi et al., 2012). Similarly, Late Triassic bimodal volcanic rocks emplaced into the SQB and NQB (e.g., Xiaoqiebao Fm. and 200–230 Ma Nadi Kangri Formation) have been interpreted to reflect an intra-plate extensional environment (Fu et al., 2010a, 2010b; Li, 2019; Wang et al., 2022), possibly associated with post-collisional extension. These inferences too would suggest that the LSO had closed at least by Late Triassic time (Figure 3e).

In summary, geological observations support the inference that the LSO had closed at least by mid-Late Triassic time (if not earlier), as suggested by paleomagnetic constraints. A more specific estimate of the closure timing of the LSO and a better understanding of its mode of closure (e.g., diachronic closure from east to west or west to east; e.g., Tang & Zhang, 2014; Lu et al., 2019; Xu et al., 2020; Y. X Zhang et al., 2018) will require additional paleomagnetic constraints from the SQB.

5. Conclusions

We have reported new paleomagnetic results from a study of Late Triassic volcanic rocks of the SQB. A ChRM derived from 25 sites passes the fold test and reversal test and likely represents a primary magnetization. These new paleomagnetic data indicate that the SQB was located at 30.1°N ± 4.6° at ~222 Ma. A consideration of these data together with other paleomagnetic and geologic constraints from neighboring continental blocks indicates that both the northern (Paleo-Jinshajiang Ocean) and southern (Longmuco-Shuanghu Ocean) branches of the Paleo-Tethys Ocean closed at a similar time, and no later than the mid-Late Triassic (~222 Ma).

Acknowledgments
We thank Editor Quentin Williams and two anonymous reviewers for their constructive comments and suggestions which greatly helped improve the manuscript. Financial support for this study was jointly provided by the National Natural Science Foundation of China (Grants 42274097, 91855211, 42304092, 42074075, and 41774073), the State Scholarship Fund, CSC, China (202306970054), the Doctoral Dissertation Cultivation Project of Northwest University (project YB2023002), the Second Tibetan Plateau Scientific Expedition (STEP) program (2019QZKK0704) and the Research Council of Norway through its Centres of Excellence funding scheme, project 223272 (Centre for Earth Evolution and Dynamics) and project 332523 (Centre for Planetary Habitability).

Data Availability Statement

Data used in this study (Tables S1 to S3) can be accessed at Zenodo (Wei, 2023).

References

Angiolini, L., Zanchi, A., Zanchetta, S., Nicora, A., & Vezzoli, G. (2013). The Cimmerian geopuzzle: New data from South Pamir. *Terra Nova*, *25*(5), 352–360. https://doi.org/10.1111/ter.12042

Besse, J., Torcq, F., Gallet, Y., Ricou, L. E., Krystyn, L., & Saidi, A. (1998). Late Permian to late Triassic palaeomagnetic data from Iran: Constraints on the migration of the Iranian block through the Tethyan Ocean and initial destruction of Pangaea. *Geophysical Journal International*, *135*(1), 77–92. https://doi.org/10.1046/j.1365-246X.1998.00603.x

Cao, Y., Sun, Z. M., Li, H. B., Pei, J. L., Liu, D. L., Zhang, L., et al. (2019). New paleomagnetic results from middle Jurassic limestones of the Qiangtang terrane, Tibet: Constraints on the evolution of the Bangong-Nujiang Ocean. *Tectonics*, *38*(1), 215–232. https://doi.org/10.1029/2017TC004842

Cao, Y., Sun, Z. M., Li, H. B., Ye, X. Z., Pan, J. W., Liu, D. L., et al. (2020). Paleomagnetism and U-Pb geochronology of early cretaceous volcanic rocks from the Qiangtang block, Tibetan Plateau: Implications for the Qiangtang-Lhasa collision. *Tectonophysics*, *789*, 228500. https://doi.org/10.1016/j.tecto.2020.228500

Chang, C. F., & Zheng, X. L. (1973). Tectonic features of the mount Jolmo Lungma region in southern Tibet, China. *Scientia Geologica Sinica*, *1*, 1–12.
Chen, W. W., Zhang, S. H., Ding, J. K., Zhang, J. H., Zhao, X. X., Zhu, L. D., et al. (2017). Combined paleomagnetic and geochronological study on Cretaceous strata of the Qiangtang terrane, central Tibet. *Gondwana Research*, *41*, 373–389. https://doi.org/10.1016/j.gr.2015.07.004
Cheng, X., Wei, B. T., Jiang, N., Zhou, Y. N., Kravchinsky, V., Chen, Q. L., et al. (2023). *Evolution of the North Qiangtang block in the late Paleozoic: Paleomagnetism and its tectonic implications*. Geological Society of America Bulletin.
Cheng, X., Wu, H. N., Guo, Q., Hou, B. N., Xia, L. Y., Wang, H. J., et al. (2012). Paleomagnetic results of late Paleozoic rocks from northern Qiangtang block in Qinghai-Tibet Plateau, China. *Science China Earth Sciences*, *55*(1), 67–75. https://doi.org/10.1007/s11430-011-4287-x
Dan, W., Wang, Q., Murphy, J. B., Zhang, X. Z., Xu, Y. G., White, W. M., et al. (2021). Short duration of early Permian Qiangtang-Panjal large igneous province: Implications for origin of the Neo-Tethys Ocean. *Earth and Planetary Science Letters*, *568*, 117054. https://doi.org/10.1016/j.epsl.2021.117054
Dan, W., Wang, Q., White, W. M., Zhang, X. Z., Tang, G. J., Jiang, Z. Q., et al. (2018). Rapid formation of eclogites during a nearly closed ocean: Revisiting the Pianshishan eclogite in Qiangtang, central Tibetan Plateau. *Chemical Geology*, *477*, 112–122. https://doi.org/10.1016/j.chemgeo.2017.12.012
Deenen, M. H., Langereis, C. G., van Hinsbergen, D. J., & Biggin, A. J. (2011). Geomagnetic secular variation and the statistics of palaeomagnetic directions. *Geophysical Journal International*, *186*(2), 509–520. https://doi.org/10.1111/j.1365-246X.2011.05050.x
Ding, L., Kapp, P., Cai, F., Garzione, C. N., Xiong, Z., Wang, H., & Wang, C. (2022). Timing and mechanisms of Tibetan Plateau uplift. *Nature Reviews Earth & Environment*, *3*(10), 652–667. https://doi.org/10.1038/s43017-022-00318-4
Ding, L., Kapp, P., & Wan, X. (2005). Paleocene–Eocene record of ophiolite obduction and initial India-Asia collision, south central Tibet. *Tectonics*, *24*(3). https://doi.org/10.1029/2004TC001729
Dong, G. C., Mo, X. X., Zhao, Z. D., Zhu, D. C., Goodman, R. C., Kong, H. L., & Wang, S. (2013). Zircon U–Pb dating and the petrological and geochemical constraints on Lincang granite in western Yunnan, China: Implications for the closure of the Paleo-Tethys Ocean. *Journal of Asian Earth Sciences*, *62*, 282–294. https://doi.org/10.1016/j.jseaes.2012.10.003
Dong, Y. S., & Li, C. (2009). Discovery of eclogite in the Guoganjianian mountain, central Qiangtang area, northern Tibet, China. *Geological Bulletin of China*, *28*(09), 1197–1200.
Fan, J. J., Li, C., Wang, M., Xie, C. M., & Xu, W. (2015). Features, provenance, and tectonic significance of Carboniferous–Permian glacial marine diamictites in the Southern Qiangtang–Baoshan block, Tibetan Plateau. *Gondwana Research*, *28*(4), 1530–1542. https://doi.org/10.1016/j.gr.2014.10.015
Feng, X. T., Zhu, T. X., Li, C., Lin, S. L., Zhang, Q. Y., Zhang, H. H., et al. (2005). Redefinition of the Upper Triassic Xiaochaka Group in the Shuanghu area, northern Tibet, China, and its geological implications. *Geological Bulletin of China*, *24*(12), 1135–1140.
Fu, X. G., Wang, J., Chen, W. B., & Feng, X. L. (2010a). Age and tectonic implications of the late Triassic Nadi Kangri volcanic rocks in the Qiangtang basin, northern Tibet. *China: Journal of Chengdu University of Technology: Science and Technology Edition*, *37*, 605–615.
Fu, X. G., Wang, J., Tan, F. W., Chen, M., & Chen, W. B. (2010b). The late Triassic rift-related volcanic rocks from eastern Qiangtang, northern Tibet (China): Age and tectonic implications. *Gondwana Research*, *17*(1), 135–144. https://doi.org/10.1016/j.gr.2009.04.010
Fu, X. G., Wang, J., Wu, T., & He, J. L. (2009). Discovery of the large-scale paleo-weathering crust in the Qiangtang basin, northern Tibet, China and its significance. *Geological Bulletin of China*, *28*(6), 696–700.
Gao, B., Chen, J. T., Qie, W. K., & Wang, X. D. (2022). Revisiting the paleogeographic framework of northeastern Gondwana in the late Paleozoic: Implications from detrital zircon analysis. *Sedimentary Geology*, *434*, 106144. https://doi.org/10.1016/j.sedgeo.2022.106144
Gehrels, G., Kapp, P., DeCelles, P., Pullen, A., Blakey, R., Weislogel, A., et al. (2011). Detrital zircon geochronology of pre-Tertiary strata in the Tibetan-Himalayan orogen. *Tectonics*, *30*(5). https://doi.org/10.1029/2011TC002868
Guan, C., Yan, M., Zhang, W. L., Zhang, D. W., Fu, Q., Yu, L., et al. (2021). Paleomagnetic and chronologic data bearing on the Permian/Triassic boundary position of Qamdo in the eastern Qiantang Terrane: Implications for the closure of the Paleo-Tethys. *Geophysical Research Letters*, *48*(6), e2020GL092059. https://doi.org/10.1029/2020GL092059
He, H. Y., Li, Y. L., Xiao, S. Q., Sui, Q. L., Zhang, H. B., Wang, T. T., et al. (2022). Triassic Paleo-Tethyan slab break-off constrained by a newly discovered 211 Ma Dacite–Rhyolite suite in the Qiangtang terrane, central Tibet. *Journal of Asian Earth Sciences*, *240*, 105444. https://doi.org/10.1016/j.jseaes.2022.105444
Heslop, D., & Roberts, A. P. (2018). Revisiting the paleomagnetic reversal test: A Bayesian hypothesis testing framework for a common mean direction. *Journal of Geophysical Research: Solid Earth*, *123*(9), 7225–7236. https://doi.org/10.1029/2018JB016081
Hu, P. Y., Li, C., Yang, H. T., Zhang, H. B., & Yu, H. (2010). Characteristic, zircon dating and tectonic significance of Late Triassic granite in the Guoganjianianshan area, central Qiangtang, Qinghai-Tibet Plateau, China. *Geological Bulletin of China*, *29*(12), 1825–1832.
Hu, P. Y., Li, C., Li, J., Wang, M., Xie, C. M., & Wu, Y. W. (2014a). Zircon U–Pb–Hf isotopes and whole-rock geochemistry of gneissic granites from the Jitang complex in Leiwuqi area, eastern Tibet, China: Record of the closure of the Paleo-Tethys Ocean. *Tectonophysics*, *623*, 83–99. https://doi.org/10.1016/j.tecto.2014.03.018
Hu, P. Y., Li, C., Wu, Y. W., Xie, C. M., Wang, M., Zhang, H. Y., & Li, J. (2014). The Silurian Tethyan Ocean in central Qiangtang, northern Tibet: Constraints from zircon U-Pb ages of plagiogranites within the Taoxinghu ophiolite. *Geological Bulletin of China*, *33*(11), 1651–1661.
Hu, X. M., Garzanti, E., Wang, J. G., Huang, W. T., An, W., & Webb, A. (2016). The timing of India-Asia collision onset–Facts, theories, controversies. *Earth-Science Reviews*, *160*, 264–299. https://doi.org/10.1016/j.earscirev.2016.07.014
Hu, X. M., Ma, A. L., Xue, W. W., Garzanti, E., Cao, Y., Li, S. M., et al. (2022). Exploring a lost ocean in the Tibetan Plateau: Birth, growth, and demise of the Bangong-Nujiang Ocean. *Earth-Science Reviews*, *229*, 104031. https://doi.org/10.1016/j.earscirev.2022.104031
Huang, B. C., Yan, Y. G., Piper, J. D. A., Zhang, D. H., Yi, Z. Y., Yu, S., & Zhou, T. H. (2018). Paleomagnetic constraints on the paleogeography of the East Asian blocks during late Paleozoic and early Mesozoic times. *Earth-Science Reviews*, *186*, 8–36. https://doi.org/10.1016/j.earscirev.2018.02.004
Huang, K., & Opdyke, N. D. (1991). Paleomagnetic results from the Upper Carboniferous of the Shan-Thai-Malay block of western Yunnan, China. *Tectonophysics*, *192*(3–4), 333–344. https://doi.org/10.1016/0040-1951(91)90107-4
Jin, C. S., Liu, Q. S., Liang, W. T., Roberts, A. P., Sun, J. M., Hu, P. X., et al. (2018). Magnetostratigraphy of the Fenghuoshan Group in the Hoh Xil basin and its tectonic implications for India–Eurasia collision and Tibetan Plateau deformation. *Earth and Planetary Science Letters*, *486*, 41–53. https://doi.org/10.1016/j.epsl.2018.01.010
Jin, X., Zhang, Y. X., Zhou, X. Y., Zhang, K. J., Li, Z. W., Khalid, S. B., et al. (2019). Protoliths and tectonic implications of the newly discovered Triassic Baqing eclogites, central Tibet: Evidence from geochemistry, SrNd isotopes and geochronology. *Gondwana Research*, *69*, 144–162. https://doi.org/10.1016/j.gr.2018.12.011
Kapp, P., DeCelles, P. G., Gehrels, G. E., Heizler, M., & Ding, L. (2007). Geological records of the Lhasa-Qiangtang and Indo-Asian collisions in the Nima area of central Tibet. *Geological Society of America Bulletin*, *119*(7–8), 917–933. https://doi.org/10.1130/B26033.1

Kapp, P., Yin, A., Manning, C. E., Harrison, T. M., Taylor, M. H., & Ding, L. (2003). Tectonic evolution of the early Mesozoic blueschist-bearing Qiangtang metamorphic belt, central Tibet. *Tectonics*, *22*(4), 1043. https://doi.org/10.1029/2002TC001383

Kapp, P., Yin, A., Manning, C. E., Murphy, M., Harrison, T. M., Spurlin, M., et al. (2000). Blueschist-bearing metamorphic core complexes in the Qiangtang block reveal deep crustal structure of northern Tibet. *Geology*, *28*(1), 19–22. https://doi.org/10.1130/0091-7613(2000)28<19:BMCCIT>2.0.CO;2

Li, C. (1987). The Longmucuo-Shuanghu-Lancangjiang plate suture and the north boundary of distribution of Gondwana facies Permo-Carboniferous system in northern Xizang. *Journal of Changchun College of Geology*, *17*, 155–166.

Li, C. (2008). A review on 20 years' study of the Longmu Co-Shuanghu-Lancang river suture zone in Qinghai-Xizang (Tibet) Plateau. *Geological Review*, *54*(1), 105–119.

Li, C., Zhai, Q. G., Dong, Y. S., Liu, S., Xie, C. M., & Wu, Y. W. (2009). High-pressure eclogite-blueschist metamorphic belt and closure of paleo-Tethys Ocean in Central Qiangtang, Qinghai-Tibet plateau. *Journal of Earth Sciences*, *20*(2), 209–218. https://doi.org/10.1007/s12583-009-0021-4

Li, C., Zhai, Q. G., Dong, Y. S., Yu, J. J., & Huang, X. P. (2007). Establishment of the Upper Triassic Wanghuling formation at Guoganjianian mountain, central Qiangtang, Qinghai–Tibet Plateau, and its significance. *Geological Bulletin of China*, *26*(8), 1003–1008.

Li, C., Zhai, Q. G., Dong, Y. S., Zeng, Q. G., & Huang, X. P. (2007). Longmu Co-Shuanghu plate suture and evolution records of Paleo-Tethyan oceanic in Qiangtang area, Qinghai-Tibet plateau. *Frontiers of Earth Science in China*, *1*(3), 257–264. https://doi.org/10.1007/s11707-007-0032-3

Li, G. M., Li, J. X., Zhao, J. X., Qin, K. Z., Cao, M. J., & Evans, N. J. (2015). Petrogenesis and tectonic setting of Triassic granitoids in the Qiangtang terrane, central Tibet: Evidence from U–Pb ages, petrochemistry and Sr–Nd–Hf isotopes. *Journal of Asian Earth Sciences*, *105*, 443–455. https://doi.org/10.1016/j.jseaes.2015.02.017

Li, S., Chung, S. L., Hou, Z. Q., Chew, D., Wang, T., Wang, B. D., & Wang, Y. B. (2019). Early Mesozoic magmatism within the Tibetan Plateau: Implications for the Paleo-Tethyan tectonic evolution and continental amalgamation. *Tectonics*, *38*(10), 3505–3543. https://doi.org/10.1029/2019TC005546

Li, X., Suzuki, N., Zhang, Y. C., Zhang, H., Luo, M., Yuan, D. X., et al. (2024). The central Qiangtang metamorphic belt in northern Tibet is an in-situ Paleo-Tethys Ocean: Evidence from newly discovered late Devonian radiolarians. *Gondwana Research*, *125*, 49–58. https://doi.org/10.1016/j.gr.2023.08.005

Li, X. R. (2019). *Volcanic-sedimentary petrological characteristics and tectonic: Attribute of Nadigangri formation in Qiangtang Basin*. China University of Geosciences.

Li, Z. Y., Ding, L., Song, P. P., Fu, J. J., & Yue, Y. H. (2017). Paleomagnetic constraints on the paleolatitude of the Lhasa block during the early Cretaceous: Implications for the onset of India–Asia collision and latitudinal shortening estimates across Tibet and stable Asia. *Gondwana Research*, *41*, 352–372. https://doi.org/10.1016/j.gr.2015.05.013

Lin, J. L., & Watts, D. R. (1988). Palaeomagnetic results from the Tibetan Plateau. *Philosophical Transactions of the Royal Society of London - Series A: Mathematical and Physical Sciences*, *327*(1594), 239–262. https://doi.org/10.1098/rsta.1988.0128

Liu, C. Y., Yang, X. K., Ren, Z. L., Lai, S. C., Chen, G., Zhao, H. G., et al. (2001). Structure framework and its evolution in Chasang area of Qiangtang basin, northern Tibet. *Science in China - Series D: Earth Sciences*, *44*(1), 18–26. https://doi.org/10.1007/BF02911967

Liu, C. Y., Yang, X. K., Wei, Y. P., Ren, Z. L., Lai, S. C., Chen, G., et al. (2002). Structure and tectonic feature of Chasang area in west part of Qiangtang basin, north part of Tibet. *Geological Review*, *48*(6), 5933602.

Liu, D. L., Shi, R. D., Ding, L., & Jiang, S. Y. (2019). Survived Seamount Reveals an in situ Origin for the central Qiangtang metamorphic belt in the Tibetan Plateau. *Journal of Earth Sciences*, *30*(6), 1253–1265. https://doi.org/10.1007/s12583-019-1250-9

Liu, F. C., Pan, J. W., Li, H. B., Sun, Z. M., Liu, D. L., Lu, H. J., et al. (2022). Characteristics of quaternary activities along the Riganpei co fault and seismogenic structure of the July 23, 2020 Mw6.4 Nima Earthquake, central Tibet. *Acta Geoscientia Sinica*, 20210108-1141.

Liu, Y. M., Wang, M., Li, C., Xie, C. M., Chen, H. Q., Li, Y. B., et al. (2017). Cretaceous structures in the Duolong region of central Tibet: Evidence for an accretionary wedge and closure of the Bangong–Nujiang Neo-Tethys Ocean. *Gondwana Research*, *48*, 110–123. https://doi.org/10.1016/j.gr.2017.04.026

Lu, L., Qin, Y., Li, Z. F., Yan, L. L., Jin, X., & Zhang, K. J. (2019). Diachronous closure of the Shuanghu Paleo-Tethys Ocean: Constraints from the late Triassic Tanggula arc-related volcanism in the East Qiangtang subterrane, central Tibet. *Lithos*, *328*, 182–199. https://doi.org/10.1016/j.lithos.2019.01.034

Ma, A. L., Hu, X. M., Garzanti, E., Pullen, A., BouDagher-Fadel, M., Ji, X. K., et al. (2023). Mid-Cretaceous exhumation of the central Qiangtang mountain range metamorphic rocks as evidenced by the Abushan Continental redbeds. *Tectonics*, *42*(3), e2022TC007520. https://doi.org/10.1029/2022TC007520

Ma, L., Liu, H., Wu, C. S., Li, Z. X., Li, Y., Wei, H. W., & Deng, Q. (2016). The age and geological significance of the Shanzixingshan volcanic rocks in Shuanghu of Northern Tibet. *4*(40), 389–395.

Ma, Y. M., Wang, Q., Wang, J., Yang, T. S., Tan, X. D., Dan, W., et al. (2019). Paleomagnetic constraints on the origin and drift history of the North Qiangtang Terrane in the late Paleozoic. *Geophysical Research Letters*, *46*(2), 689–697. https://doi.org/10.1029/2018GL080964

McFadden, P. L., & Mcelhinny, M. W. (1990). Classification of the reversal test in paleomagnetism. *Geophysical Journal International*, *103*(3), 725–729. https://doi.org/10.1111/j.1365-246X.1990.tb05683.x

Meng, J., Zhao, X. X., Wang, C. S., Liu, H., Li, Y. L., Han, Z. P., et al. (2018). Palaeomagnetism and detrital zircon U–Pb geochronology of Cretaceous redbeds from central Tibet and tectonic implications. *Geological Journal*, *53*(5), 2315–2333. https://doi.org/10.1002/gj.3070

Metcalfe, I. (2013). Gondwana dispersion and Asian accretion: Tectonic and palaeogeographic evolution of eastern Tethys. *Journal of Asian Earth Sciences*, *66*, 1–33. https://doi.org/10.1016/j.jseaes.2012.12.020

Pan, G. T., Zhu, D. C., Wang, L. Q., Liao, Z. L., Geng, Q. R., & Jiang, X. S. (2004). Bangong Lake—Nu River suture zone the northern boundary of Gondwanaland：Evidence from geology and geophysics. *Earth Science Frontiers*, *11*(4), 371–382.

Peng, T. P., Zhao, G. C., Fan, W. M., Peng, B. X., & Mao, Y. S. (2015). Late Triassic granitic magmatism in the eastern Qiangtang, eastern Tibetan Plateau: Geochronology, petrogenesis and implications for the tectonic evolution of the Paleo-Tethys. *Gondwana Research*, *27*(4), 1494–1508. https://doi.org/10.1016/j.gr.2014.01.009

Pullen, A., Kapp, P., Gehrels, G. E., Ding, L., & Zhang, Q. (2011). Metamorphic rocks in central Tibet: Lateral variations and implications for crustal structure. *Geological Society of America Bulletin*, *123*(3–4), 585–600. https://doi.org/10.1130/B30154.1

Pullen, A., Kapp, P., Gehrels, G. E., Vervoort, J. D., & Ding, L. (2008). Triassic continental subduction in central Tibet and Mediterranean-style closure of the Paleo-Tethys Ocean. *Geology*, *36*(5), 351–354. https://doi.org/10.1130/G24435A.1

Qi, S. S., Wang, Y. Z., He, S. H., Song, S. C., Qi, Z. L., & Wang, F. L. (2009). The assurance of syncollisional granite in tanggula Area during late Permian epoch and its significance. *Northwestern Geology*, *42*(3), 26–35.

Qian, X., Wang, Y. J., Feng, Q. L., Zi, J. W., Zhang, Y. Z., & Chonglakmani, C. (2016). Petrogenesis and tectonic implication of the Late Triassic post-collisional volcanic rocks in Chiang Khong, NW Thailand. *Lithos*, *248*, 418–431. https://doi.org/10.1016/j.lithos.2016.01.024

Ren, Z. L., Cui, J. P., Liu, C. Y., Li, T. J., Chen, G., Chen, Z. J., et al. (2016). Uplift and cooling history of Qiangtang Basin and its significance. *Petroleum Geology and Experiment*, *38*(1), 15–22.

Şengör, A. M. C., Altıner, D., Cin, A., Ustaömer, T., & Hsü, K. J. (1988). Origin and assembly of the Tethyside orogenic collage at the expense of Gondwana Land. *Geological Society, London, Special Publications*, *37*(1), 119–181. https://doi.org/10.1144/GSL.SP.1988.037.01.09

Shen, S. Z., Sun, T. R., Zhang, Y. C., & Yuan, D. X. (2016). An upper Kungurian/lower Guadalupian (Permian) brachiopod fauna from the South Qiangtang block in Tibet and its palaeobiogeographical implications. *Palaeoworld*, *25*(4), 519–538. https://doi.org/10.1016/j.palwor.2016.03.006

Shi, C., Li, R. S., He, S. P., Wang, C., Pan, S. J., Zhang, H. D., & Gu, P. Y. (2012). Zircon U–Pb dating, geochemical and geological significances studies for gneissic biotite monzogranite in Riwoqe County, Tibet. *Xinjiang Geology*, *30*(4), 456–464.

Song, C. Y., Wang, J., Fu, X. G., Feng, X. L., Chen, M., & He, L. (2012). Late Triassic Paleomagnetic data from the Qiangtang terrane of Tibetan Plateau and their tectonic significances. *Journal of Jilin University (Earth Science Edition)*, *42*(2), 526–535.

Song, P. P., Ding, L., Li, Z. Y., Lippert, P. C., Yang, T. S., Zhao, X. X., et al. (2015). Late Triassic paleolatitude of the Qiangtang block: Implications for the closure of the Paleo-Tethys Ocean. *Earth and Planetary Science Letters*, *424*, 69–83. https://doi.org/10.1016/j.epsl.2015.05.020

Song, P. P., Ding, L., Li, Z., Lippert, P. C., & Yue, Y. H. (2017). An early bird from Gondwana: Paleomagnetism of lower Permian lavas from northern Qiangtang (Tibet) and the geography of the Paleo-Tethys. *Earth and Planetary Science Letters*, *475*, 119–133. https://doi.org/10.1016/j.epsl.2017.07.023

Stampfli, G. M., & Borel, G. D. (2002). A plate tectonic model for the Paleozoic and Mesozoic constrained by dynamic plate boundaries and restored synthetic oceanic isochrons. *Earth and Planetary Science Letters*, *196*(1–2), 17–33. https://doi.org/10.1016/S0012-821X(01)00588-X

Stampfli, G. M., Hochard, C., Vérard, C., Wilhem, C., & von Raumer, J. (2013). The formation of Pangea. *Tectonophysics*, *593*, 1–19. https://doi.org/10.1016/j.tecto.2013.02.037

Suo, Y. H., Li, S. Z., Cao, X. Z., Dong, H., Li, X. Y., & Wang, X. Y. (2022). Two-stage eastward diachronous model of India-Eurasia collision: Constraints from the intraplate tectonic records in Northeast Indian Ocean. *Gondwana Research*, *102*, 372–384. https://doi.org/10.1016/j.gr.2020.01.006

Tang, X. C., & Zhang, K. J. (2014). Lawsonite-and glaucophane-bearing blueschists from NW Qiangtang, northern Tibet, China: Mineralogy, geochemistry, geochronology, and tectonic implications. *International Geology Review*, *56*(2), 150–166. https://doi.org/10.1080/00206814.2013.820866

Torsvik, T. H., & Cocks, L. R. M. (2013). Gondwana from top to base in space and time. *Gondwana Research*, *24*(3–4), 999–1030. https://doi.org/10.1016/j.gr.2013.06.012

Torsvik, T. H., Van der Voo, R., Preeden, U., Mac Niocaill, C., Steinberger, B., Doubrovine, P. V., et al. (2012). Phanerozoic polar wander, palaeogeography and dynamics. *Earth-Science Reviews*, *114*(3–4), 325–368. https://doi.org/10.1016/j.earscirev.2012.06.007

Wan, B., Chu, Y., Chen, L., Liang, X. F., Zhang, Z. Y., Ao, S. J., & Talebian, M. (2021). Paleo-Tethys subduction induced slab-drag opening the Neo-Tethys: Evidence from an Iranian segment of Gondwana. *Earth-Science Reviews*, *221*, 103788. https://doi.org/10.1016/j.earscirev.2021.103788

Wan, B., Wu, F. Y., Chen, L., Zhao, L., Liang, X. F., Xiao, W. J., & Zhu, R. X. (2019). Cyclical one-way continental rupture-drift in the Tethyan evolution: Subduction-driven plate tectonics. *Science China Earth Sciences*, *62*(12), 2005–2016. https://doi.org/10.1007/s11430-019-9393-4

Wang, B. D., Wang, L. Q., Qiangba, Z. X., Zeng, Q. G., Zhang, W. P., Wang, D. B., & Cheng, W. H. (2011). Early Triassic collision of northern Lancangjiang suture: Geochronological, geochemical and Hf isotope evidences from the granitic gneiss in Leiwuqi area, East Tibet. *Acta Petrologica Sinica*, *27*(9), 2752–2762.

Wang, C. M., Deng, J., Santosh, M., Lu, Y. J., McCuaig, T. C., Carranza, E. J. M., & Wang, Q. F. (2015). Age and origin of the Bulangshan and Mengsong granitoids and their significance for post-collisional tectonics in the Changning–Menglian Paleo-Tethys Orogen. *Journal of Asian Earth Sciences*, *113*, 656–676. https://doi.org/10.1016/j.jseaes.2015.05.001

Wang, J., Fu, X. G., Chen, W. X., & Wang, Z. J. (2007). The late Triassic paleo-weathering crust in the Qiangtang basin, northern Tibet: Geology, geochemistry and significance. *Acta Sedimentologica Sinica*, *25*(4), 487.

Wang, J., & Fu, X. G. (2018). Sedimentary evolution of the Qiangtang Basin. *Geology in China*, *45*(2), 237–259.

Wang, J., Fu, X. G., Wei, H. Y., Shen, L. J., Wang, Z., & Li, K. Z. (2022). Late Triassic basin inversion of the Qiangtang Basin in northern Tibet: Implications for the closure of the Paleo-Tethys and expansion of the Neo-Tethys. *Journal of Asian Earth Sciences*, *227*, 105119. https://doi.org/10.1016/j.jseaes.2022.105119

Wang, M., Li, C., Zeng, X. W., Li, H., Fan, J. J., Xie, C. M., & Hao, Y. J. (2019). Petrogenesis of the southern Qiangtang mafic dykes, Tibet: Link to a late Paleozoic mantle plume on the northern margin of Gondwana? *Geological Society of America Bulletin*, *131*(11–12), 1907–1919. https://doi.org/10.1130/B35110.1

Wang, Q., Zhu, D. C., Cawood, P. A., Chung, S. L., & Zhao, Z. D. (2021). Resolving the paleogeographic puzzle of the Lhasa Terrane in southern Tibet. *Geophysical Research Letters*, *48*(15), e2021GL094236. https://doi.org/10.1029/2021GL094236

Wang, Y. J., Qian, X., Cawood, P. A., Liu, H. C., Feng, Q. L., Zhao, G. C., et al. (2018). Closure of the East Paleotethyan Ocean and amalgamation of the Eastern Cimmerian and Southeast Asia continental fragments. *Earth-Science Reviews*, *186*, 195–230. https://doi.org/10.1016/j.earscirev.2017.09.013

Wang, Y. S., Qu, Y. G., Sun, Z. G., Zheng, C. Z., Xie, Y. H., & Lu, Z. L. (2007). Characteristics and tectonic setting of volcanic rocks of the Triassic Nongbo Formation at the northern margin of the south Qiangtang block, northern Tiber, China. *Geological Bulletin of China*, *26*(6), 682–691.

Watson, G. S., & Enkin, R. J. (1993). The fold test in paleomagnetism as a parameter estimation problem. *Geophysical Research Letters*, *20*(19), 2135–2137. https://doi.org/10.1029/93GL01901

Wei, B. T. (2023). Paleomagnetism of late Triassic volcanic rocks from the south Qiangtang block, Tibet: Constrains on Longmuco-Shuanghu Ocean closure in the Paleo-Tethys Realm [Dataset]. Zenodo. https://doi.org/10.5281/zenodo.8332299

Wei, B. T., Cheng, X., Domeier, M., Jiang, N., Wu, Y. Y., Zhang, W. J., et al. (2022). Placing another piece of the Tethyan puzzle: The first Paleozoic paleomagnetic data from the South Qiangtang block and its paleogeographic implications. *Tectonics*, *41*(10), e2022TC007355. https://doi.org/10.1029/2022TC007355

Wu, F. Y., Wan, B., Zhao, L., Xiao, W. J., & Zhu, R. X. (2020). Tethyan geodynamics. *Acta Petrologica Sinica*, *36*(6), 1627–1674. https://doi.org/10.18654/1000-0569/2020.06.01

Wu, Z. H., Ye, P. S., Barosh, P. J., Hu, D. G., Lu, L., & Zhang, Y. L. (2012). Early Cenozoic mega thrusting in the Qiangtang block of the northern Tibetan Plateau. *Acta Geologica Sinica-English Edition*, *86*(4), 799–809. https://doi.org/10.1111/j.1755-6724.2012.00707.x

Wu, Z. H., Ye, P. S., Hu, D. G., & Chen, L. (2011). Paleogene thrust system in southern Qiangtang basin, central Tibetan Plateau. *Geological Bulletin of China*, *30*(7), 1009–1016.

Xie, C. M., Li, C., Ren, Y. S., Wang, M., & Su, L. (2018). Detrital provenance, depositional environment, and palaeogeographic implications of Lower Triassic marine sediments in central Tibet. *International Geology Review*, *60*(4), 418–430. https://doi.org/10.1080/00206814.2017.1336945

Xu, W., Liu, F., & Dong, Y. (2020). Cambrian to Triassic geodynamic evolution of central Qiangtang, Tibet. *Earth-Science Reviews*, *201*, 103083. https://doi.org/10.1016/j.earscirev.2020.103083

Xu, Y. C., Yang, Z. Y., Tong, Y. B., Wang, H., Gao, L., & An, C. Z. (2015). Further paleomagnetic results for lower Permian basalts of the Baoshan Terrane, southwestern China, and paleogeographic implications. *Journal of Asian Earth Sciences*, *104*, 99–114. https://doi.org/10.1016/j.jseaes.2014.10.029

Yan, M. D., Zhang, D. W., Fang, X. M., Ren, H. D., Zhang, W. L., Zan, J. B., et al. (2016). Paleomagnetic data bearing on the Mesozoic deformation of the Qiangtang block: Implications for the evolution of the Paleo-and Meso-Tethys. *Gondwana Research*, *39*, 292–316. https://doi.org/10.1016/j.gr.2016.01.012

Yan, Y. G., Duan, L., Liang, S. M., Wang, J. H., Huang, B. C., Zheng, W. J., & Zhang, P. Z. (2020). Paleomagnetic constraint on the Carboniferous paleoposition of Indochina and its implications for the evolution of eastern Paleo-Tethys Ocean. *Tectonics*, *39*(7), e2020TC006168. https://doi.org/10.1029/2020TC006168

Yan, Y. G., Zhao, Q., Zhang, Y. P., Huang, B. C., Zheng, W. J., & Zhang, P. Z. (2019). Direct paleomagnetic constraint on the closure of Paleo-Tethys and its implications for linking the Tibetan and Southeast Asian blocks. *Geophysical Research Letters*, *46*(24), 14368–14376. https://doi.org/10.1029/2019GL085473

Yang, T. N., Zhang, H. R., Liu, Y. X., Wang, Z. L., Song, Y. C., Yang, Z. S., et al. (2011). Permo-Triassic arc magmatism in central Tibet: Evidence from zircon U–Pb geochronology, Hf isotopes, rare earth elements, and bulk geochemistry. *Chemical Geology*, *284*(3–4), 270–282. https://doi.org/10.1016/j.chemgeo.2011.03.006

Yang, X. F., Cheng, X., Zhou, Y. N., Ma, L., Zhang, X. D., Yan, Z. S., et al. (2017). Paleomagnetic results from late carboniferous to early Permian rocks in the northern Qiangtang terrane, Tibet, China, and their tectonic implications. *Science China Earth Sciences*, *60*(001), 124–134. https://doi.org/10.1007/s11430-015-5462-7

Yin, A., & Harrison, T. M. (2000). Geologic evolution of the Himalayan-Tibetan orogen. *Annual Review of Earth and Planetary Sciences*, *28*(1), 211–280. https://doi.org/10.1146/annurev.earth.28.1.211

Yu, L., Yan, M. D., Domeier, M., Guan, C., Shen, M. M., Fu, Q., et al. (2022). New paleomagnetic and chronological constraints on the late triassic position of the eastern Qiangtang terrane: Implications for the closure of the Paleo-Jinshajiang Ocean. *Geophysical Research Letters*, *49*(2), e2021GL096902. https://doi.org/10.1029/2021GL096902

Zhai, Q. G., Zhang, R. Y., Jahn, B. M., Li, C., Song, S. G., & Wang, J. (2011). Triassic eclogites from central Qiangtang, northern Tibet, China: Petrology, geochronology and metamorphic P–T path. *Lithos*, *125*(1–2), 173–189. https://doi.org/10.1016/j.lithos.2011.02.004

Zhai, Q. G., Jahn, B. M., Li, X. H., Zhang, R. Y., Li, Q. L., Yang, Y. N., et al. (2017). Zircon U–Pb dating of eclogite from the Qiangtang terrane, north-central Tibet: A case of metamorphic zircon with magmatic geochemical features. *International Journal of Earth Sciences*, *106*(4), 1239–1255. https://doi.org/10.1007/s00531-016-1418-9

Zhai, Q. G., Jahn, B. M., Su, L., Ernst, R. E., Wang, K. L., Zhang, R. Y., et al. (2013). SHRIMP zircon U–Pb geochronology, geochemistry and Sr–Nd–Hf isotopic compositions of a mafic dyke swarm in the Qiangtang terrane, northern Tibet and geodynamic implications. *Lithos*, *174*, 28–43. https://doi.org/10.1016/j.lithos.2012.10.018

Zhai, Q. G., Jahn, B. M., Wang, J., Hu, P. Y., Chung, S. L., Lee, H. Y., et al. (2016). Oldest paleo-Tethyan ophiolitic mélange in the Tibetan Plateau. *GSA Bulletin*, *128*(3–4), 355–373. https://doi.org/10.1130/B31296.1

Zhai, Q. G., Jahn, B. M., Wang, J., Su, L., Mo, X. X., Wang, K. L., et al. (2013). The Carboniferous ophiolite in the middle of the Qiangtang terrane, northern Tibet: SHRIMP U–Pb dating, geochemical and Sr–Nd–Hf isotopic characteristics. *Lithos*, *168*, 186–199. https://doi.org/10.1016/j.lithos.2013.02.005

Zhai, Q. G., Wang, J., Hu, P. Y., Lee, H. Y., Tang, Y., Wang, H. T., et al. (2018). Late Paleozoic granitoids from central Qiangtang, northern Tibetan plateau: A record of Paleo-Tethys Ocean subduction. *Journal of Asian Earth Sciences*, *167*, 139–151. https://doi.org/10.1016/j.jseaes.2017.07.030

Zhang, K. J., Cai, J. X., Zhang, Y. X., & Zhao, T. P. (2006). Eclogites from central Qiangtang, northern Tibet (China) and tectonic implications. *Earth and Planetary Science Letters*, *245*(3–4), 722–729. https://doi.org/10.1016/j.epsl.2006.02.025

Zhang, K. J., & Tang, X. C. (2009). Eclogites in the interior of the Tibetan Plateau and their geodynamic implications. *Chinese Science Bulletin*, *54*(15), 2556–2567. https://doi.org/10.1007/s11434-009-0407-9

Zhang, K. J., Zhang, Y. X., Li, B., Zhu, Y. T., & Wei, R. Z. (2006). The blueschist-bearing Qiangtang metamorphic belt (northern Tibet, China) as an in situ suture zone: Evidence from geochemical comparison with the Jinsa suture. *Geology*, *34*(6), 493–496. https://doi.org/10.1130/G22404.1

Zhang, T. Y., Fan, J. J., Li, C., Xie, C. M., Wang, M., Wu, Y. W., et al. (2018). Early Carboniferous ophiolite in central Qiangtang, northern Tibet: Record of an oceanic back-arc system in the Palaeo-Tethys Ocean. *International Geology Review*, *60*(4), 449–463. https://doi.org/10.1080/00206814.2017.1342569

Zhang, X. Z., Dong, Y. S., Li, C., Chen, W., Shi, J. R., Zhang, Y., & Wang, Y. S. (2010). Identification of the eclogites with different ages and their tectonic significance in central Qiangtang, Tibetan Plateau: Constraints from 40Ar-39Ar geochronology. *Geological Bulletin of China*, *29*(12), 1815–1824.

Zhang, X. Z., Dong, Y. S., Wang, Q., & Dan, W. (2018). High pressure metamorphic belt in central Qiangtang, Tibetan Plateau: Progress and unsolved problems. *Geological Bulletin of China*, *37*(8), 1406–1416.

Zhang, X. Z., Dong, Y. S., Wang, Q., Dan, W., Zhang, C. F., Deng, M. R., et al. (2016). Carboniferous and Permian evolutionary records for the Paleo-Tethys Ocean constrained by newly discovered Xiangtaohu ophiolites from central Qiangtang, central Tibet. *Tectonics*, *35*(7), 1670–1686. https://doi.org/10.1002/2016TC004170

Zhang, Y. C., Shen, S. Z., Zhai, Q. G., Zhang, Y. J., & Yuan, D. X. (2016). Discovery of a Sphaeroschwagerina fusuline fauna from the Raggyorcaka lake area, northern Tibet: Implications for the origin of the Qiangtang metamorphic belt. *Geological Magazine*, *153*(3), 537–543. https://doi.org/10.1017/S0016756815000795

Zhang, Y. C., Shi, G. R., Shen, S. Z., & Yuan, D. X. (2014). Permian Fusuline fauna from the lower Part of the Lugu formation in the central Qiangtang block and its geological implications. *Acta Geologica Sinica-English Edition*, *88*(2), 365–379. https://doi.org/10.1111/1755-6724.12202

Zhang, Y. X., Jin, X., Zhang, K. J., Sun, W. D., Liu, J. M., Zhou, X. Y., & Yan, L. L. (2018). Newly discovered late Triassic Baqing eclogite in central Tibet indicates an anticlockwise west–east Qiangtang collision. *Scientific Reports*, *8*(1), 966. https://doi.org/10.1038/s41598-018-19342-w

Zhao, G. C., Wang, Y. J., Huang, B. C., Dong, Y. P., Li, S. Z., Zhang, G. W., & Yu, S. (2018). Geological reconstructions of the East Asian blocks: From the breakup of Rodinia to the assembly of Pangea. *Earth-Science Reviews*, *186*, 262–286. https://doi.org/10.1016/j.earscirev.2018.10.003

Zhao, Z., Lu, L., & Wu, Z. H. (2019a). Uplifting evolution of the central Uplift belt, Qiangtang: Constraints from tectono-thermochronology. *Earth Science Frontiers*, *26*(2), 249. https://doi.org/10.13745/j.esf.sf.2018.9.7

Zhao, Z., Wu, Z. H., Yu, J. Q., & Wu, Y. J. (2019b). Thrust structures of the Nima-Rongma area in the Qiangtang block, Tibetan Plateau. *Acta Geologica Sinica*, *93*(8), 1849–1866.

Zhou, Y. N., Cheng, X., Wu, Y. Y., Kravchinsky, V., Shao, R. Q., Zhang, W. J., et al. (2019). The northern Qiangtang block rapid drift during the Triassic Period: Paleomagnetic evidence. *Geoscience Frontiers*, *10*(6), 2313–2327. https://doi.org/10.1016/j.gsf.2019.05.003

Zhu, R. X., Zhao, P., Wan, B., & Sun, W. D. (2023). Geodynamics of the one-way subduction of the Neo-Tethys Ocean. *Chinese Science Bulletin*, *68*(13), 1699–1708. https://doi.org/10.1360/TB-2022-1141

Zhu, R. X., Zhao, P., & Zhao, L. (2022). *Tectonic evolution and geodynamics of the Neo-Tethys Ocean* (pp. 1–24). Science China Earth Sciences. https://doi.org/10.1007/s11430-021-9845-7

Zhu, T. X., Dong, H., Li, C., Feng, X. T., Li, Z. L., Yu, Y. S., et al. (2005). Distribution and sedimentary model of the late Triassic strata in northern Qiangtang on the Qinghai-Xizang Plateau. *Sedimentary Geology and Tethyan Geology*, *25*, 18–23.

Zhu, Z. C., Zhai, Q. G., Hu, P. Y., Tang, Y., Wang, H. T., Wang, W., & Wu, H. (2022). Resolving the timing of Lhasa-Qiangtang block collision: Evidence from the lower cretaceous duoni formation in the baingoin foreland basin. *Palaeogeography, Palaeoclimatology, Palaeoecology*, *595*, 110956. https://doi.org/10.1016/j.palaeo.2022.110956

References From the Supporting Information

Chi, C. T., Geissman, J. W., Quy, H. V., Anh, T. V., & Dung, N. T. P. (2016). Paleomagnetism of upper Permian basaltic rocks of cam Thuy formation from Thuan Chau locality, Son La, northwest Vietnam. *Vietnam Journal of Earth Sciences*, *37*(4), 289–298. https://doi.org/10.15625/0866-7187/37/4/8057

Cogné, J. P. (2003). PaleoMac: A Macintosh™ application for treating paleomagnetic data and making plate reconstructions. *Geochemistry, Geophysics, Geosystems*, *4*(1), 1007. https://doi.org/10.1029/2001GC000227

Enkin, R. J. (1994). A computer program package for analysis and presentation of paleomagnetic data. In *Pacific geoscience centre*. Geological Survey of Canada.

Fisher, R. A. (1953). Dispersion on a sphere. *Proceedings of the Royal Society of London. Series A*, *217*(1130), 295–305. https://doi.org/10.1098/rspa.1953.0064

Gallet, Y., Krystyn, L., Besse, J., Saidi, A., & Ricou, L. E. (2000). New constraints on the Upper Permian and lower Triassic geomagnetic polarity timescale from the Abadeh section (central Iran). *Journal of Geophysical Research*, *105*(B2), 2805–2815. https://doi.org/10.1029/1999JB900218

Kirschvink, J. L. (1980). The least-squares line and plane and the analysis of palaeomagnetic data. *Geophysical Journal International*, *62*(3), 699–718. https://doi.org/10.1111/j.1365-246X.1980.tb02601.x

McElhinny, M. W. (1964). Statistical significance of the fold test in palaeomagnetism. *Geophysical Journal International*, *8*(3), 338–340. https://doi.org/10.1111/j.1365-246X.1964.tb06300.x

McFadden, P. L. (1990). A new fold test for palaeomagnetic studies. *Geophysical Journal International*, *103*(1), 163–169. https://doi.org/10.1111/j.1365-246X.1990.tb01761.x

Song, P. P., Ding, L., Lippert, P. C., Li, Z. Y., Zhang, L. Y., & Xie, J. (2020). Paleomagnetism of middle Triassic lavas from northern Qiangtang (Tibet): Constraints on the closure of the Paleo-Tethys Ocean. *Journal of Geophysical Research: Solid Earth*, *125*(2), e2019JB017804. https://doi.org/10.1029/2019JB017804

Tauxe, L., Shaar, R., Jonestrask, L., Swanson-Hysell, N. L., Minnett, R., Koppers, A. A. P., et al. (2016). PMAGPY: Software package for paleomagnetic data analysis and a bridge to the magnetics information consortium (magic) database. *Geochemistry, Geophysics, Geosystems*, *17*(6), 2450–2463. https://doi.org/10.1002/2016GC006307

Van der Voo, R. (1990). The reliability of paleomagnetic data. *Tectonophysics*, *184*(1), 1–9. https://doi.org/10.1016/0040-1951(90)90116-P

Yan, Y. G., Huang, B. C., Zhao, J., Zhang, D. H., Liu, X. H., Charusiri, P., & Veeravinantanakul, A. (2017). Large southward motion and clockwise rotation of Indochina throughout the Mesozoic: Paleomagnetic and detrital zircon U–Pb geochronological constraints. *Earth and Planetary Science Letters*, *459*, 264–278. https://doi.org/10.1016/j.epsl.2016.11.035

Zhao, J., Huang, B. C., Yan, Y. G., Bai, Q. H., Dong, Y. P., Win, Z., et al. (2019). A palaeomagnetic study of the middle Permian and middle Triassic limestones from Shan State, Myanmar: Implications for collision of the Sibumasu Terrane and Indochina Terrane. *Geological Journal*, *55*(2), 1179–1194. https://doi.org/10.1002/gj.3482

Zhou, Y. N., Cheng, X., Yu, L., Yang, X. F., Su, H. L., Peng, X. M., et al. (2016). Paleomagnetic study on the Triassic rocks from the Lhasa Terrane, Tibet, and its paleogeographic implications. *Journal of Asian Earth Sciences*, *121*, 108–119. https://doi.org/10.1016/j.jseaes.2016.02.006

Zijderveld, J. D. A. (1967). A. C. demagnetization of rocks: Analysis of results. In D. W. Collinson, K. M. Creer, & S. K. Runcorn (Eds.), *Methods in paleomagnetism* (pp. 254–286). Elsevier.